

# Structural characterizations of magnetron sputtered nanocrystalline TiN thin films

Vipin Chawla<sup>a</sup>, R. Jayaganthan<sup>a,\*</sup>, Ramesh Chandra<sup>b</sup>

<sup>a</sup>Department of Metallurgical and Materials Engineering and Centre of Nanotechnology, Indian Institute of Technology Roorkee, Roorkee-247667, India

<sup>b</sup>Institute Instrumentation Center and Centre of Nanotechnology Indian Institute of Technology Roorkee, Roorkee-247667, India

## ARTICLE DATA

### Article history:

Received 25 July 2007

Accepted 13 August 2007

### Keywords:

TiN thin films

Characterization

Microstructure

## ABSTRACT

Nanocrystalline TiN thin films were deposited on Si(111) substrates by DC-magnetron sputtering. The effect of deposition temperature and time on the microstructural morphologies of the thin films was characterized by using FE-SEM and AFM. The texture of the TiN films was characterized by XRD. The films deposited under an Ar+N<sub>2</sub> atmosphere initially exhibited a (200) preferred orientation, which subsequently changed to a mixed (111)–(200) orientation with increasing deposition time at 500 °C. The films deposited under a pure N<sub>2</sub> atmosphere showed an initial (111) preferred orientation which was then transformed into a mixed (200)–(111) orientation with increasing deposition time. The changes in texture in the TiN thin films are due to one or a combination of factors such as strain energy, surface free energy, surface diffusivity and adatom mobility; the influence of each factor depends on the processing conditions. The grain size of TiN films was measured by XRD. A pyramidal shape and a columnar grain morphology were observed for TiN thin films deposited in Ar+N<sub>2</sub> (70:30) and pure N<sub>2</sub> atmosphere, respectively, as seen from the FE-SEM analysis. The average surface roughness was calculated from AFM images of the thin films; these results indicated that the average surface roughness was less for the films deposited in pure N<sub>2</sub> than for the films deposited in a mixed Ar+N<sub>2</sub> atmosphere.

© 2007 Elsevier Inc. All rights reserved.

## 1. Introduction

TiN thin films are extensively used for tribological and diffusion barrier applications due to their superior hardness and chemical stability. Nanocrystalline TiN thin films possess enhanced hardness and strength [1–3] as compared to the bulk microcrystalline thin film-form due to the nanoscale size and interface effects. The control of microstructural characteristics such as grain size, shape, textures, porosity, density, and packing factor are vital for ensuring the reliability of TiN thin films in structural and functional applications. Physical vapor deposition (PVD) techniques such as magnetron sputtering, filtered cathodic arc, ion plating, and plasma-based ion implantation are employed to deposit TiN thin films. The process parameters and heat

treatments used in PVD techniques affect the microstructural features of the TiN thin films. For example, in magnetron sputtering, the deposition parameters such as substrate temperature, pressure, target power, substrate bias, and energy and flux of bombarding particles utilized for growing the films are known to influence grain growth and crystallographic texture, which affect the resulting microstructure and properties of the films. Structure zone models [4–6] describe the microstructure of as deposited films. These models provide a qualitative picture of the expected microstructure of the films with respect to temperature. At low deposition temperatures, the films show an open columnar structure with extended voids along column boundaries. The columns are composed of smaller equiaxed grains. The voids become filled with an increase in film growth

\* Corresponding author. Tel.: +91 1332 285869; fax: +91 1332 285243.

E-mail address: rjayafmt@iitr.ernet.in (R. Jayaganthan).

temperature and form a true columnar structure, in which elongated grains are observed. The boundary between these two structural zones is depicted as  $T_s/T_m=0.3$  where,  $T_m$  is the melting point of the film. However, the transition between structural zones does not occur abruptly as it ignores the strong dependence of nucleation and growth kinetics affected by substrate structure and orientation, film growth rate, and the presence of impurities.

U. Helmersson et al. [7] have investigated the microstructural evolution in TiN films (4  $\mu\text{m}$ -thick) reactively sputter-deposited on multiphase substrates, and reported a dense columnar morphology in the films. The adatom surface diffusivities influence the growth process at all growth temperatures. The average grain size near the substrate was found to be twice as large as that of the constituent phases present in the multiphase substrate. Secondary recrystallisation and grain growth was not observed at the growth temperature investigated in their work. The grain boundaries were found to be immobile and nucleation kinetics were strongly enhanced by adatom surface diffusion. Johansson et al. [8] reported that the annealing out of growth-related mechanical defects occurs in the epitaxial films only at substrate temperature above 650 °C. J. Greene [9] investigated the microstructural evolution and surface morphological evolution at the atomic scale during the growth of polycrystalline TiN, prepared by sputter deposition, using HR-TEM, XRD, and SEM. At low deposition temperatures ( $T < 450$  °C), the films exhibited a columnar grain morphology with the preferential orientation of (111) textured grains. However, high temperature deposition resulted in non-competitive growth with a fully dense (200) orientation in the initial monolayer of the film.

Nanocomposite TiN-TiB<sub>2</sub> films, investigated by XRD and HRTEM, revealed that TiN exhibits a (111) preferred orientation which subsequently changes into a mixed (111)–(200) orientation with the addition of boron [10,11]. Kim et al. [12] have characterized RF-magnetron sputtered nanocrystalline thin TiN films (0.7  $\mu\text{m}$ ) by HR-TEM and observed the formation of fine grains in the films with an increase in flow rate of N<sub>2</sub> gas. The columnar structure perpendicular to the Si substrate surface and 5–10 nm diameter nanocrystals were found. A reduction of grain size with increase in N<sub>2</sub>/Ar ratio was observed during the film growth stage. For TiN films grown at relatively low substrate temperature ( $T_s < 0.3 T_m$ ), the crystallographic texture changed with increasing film thickness; an initial random orientation, followed by a (200) preferred orientation, has been reported in 5–10 nm thick films [13–15]. This orientation gradually transformed into (111), (220), or a mixed (111) and (220) texture depending upon the deposition conditions. R. Chandra et al. [16] studied the structural, optical and electronic properties of nanocrystalline TiN thin films deposited by DC magnetron sputtering. They observed a preferred orientation of mixed (200) and (111) for films deposited in pure N<sub>2</sub> and Ar+N<sub>2</sub> atmospheres, respectively, at low temperature. J. H. Huang et al. [17] reported the effect of nitrogen flow rate on the structure and properties of nanocrystalline TiN thin films produced by unbalanced magnetron sputtering. The (111) preferred orientation was observed initially and then changed to (200) with an increase in nitrogen flow rate.

It is well known that the texture evolution mechanisms in TiN thin films are influenced by such factors as strain energy,

surface free energy, surface diffusivity, adatom mobility; the influence of each varies as a function of processing parameters [9]. The potential application of nanocrystalline TiN films for tribological and microelectronic device applications could be successfully realized only if thorough insight is gained with regard to means to achieve the formation of desired microstructures through appropriate process controls. Owing to the aforementioned facts, the present work has focused on the characterization of the microstructural features of nanocrystalline TiN films deposited by DC-Magnetron sputtering.

## 2. Experimental

### 2.1. Deposition of TiN Films

TiN thin films were deposited on Si (111) substrates by DC magnetron sputtering. The substrate was cleaned by rinsing in ultrasonic baths of acetone and methanol and dried under nitrogen gas. The sputtering target was a 99.99% pure Ti disc (2-in. diameter and 5 mm thick). The base pressure was lower than  $2 \times 10^{-6}$  Torr and the sputtering was carried out in Ar+N<sub>2</sub> (70:30) and pure N<sub>2</sub> atmospheres. Before starting the deposition, the target was pre-sputtered for 15 min with a shutter located between the target and the substrate. During all depositions the target-to-substrate distance and sputtering power were kept fixed at 50 mm and 200 W, respectively. The TiN films were prepared for different deposition times at a 10 mTorr working pressure at 500 °C.

XRD (Bruker AXS) measurements were made using CuK $\alpha$  radiation to characterize the TiN thin films. The scan rate used was 1°/min and the scan range was from 35 to 45°. The grain size of the thin films was estimated from the Scherrer formula, as given in Eq. (1). In this expression, the grain size  $D$  is along the surface normal direction, which is also the direction of the XRD diffraction vector.

$$D = \frac{0.9\lambda}{B\cos\theta} \quad (1)$$

where  $B$  is the corrected full-width at half maximum (FWHM) of a Bragg peak,  $\lambda$  is the X-ray wavelength, and  $\theta$  is the Bragg angle.  $B$  is obtained from the equation  $B^2 = B_r^2 - B_{\text{strain}}^2 - C^2$  [18], where  $B_r$  is the FWHM of a measured Bragg peak,  $B_{\text{strain}} = \epsilon \tan \theta$  is the lattice broadening from the residual strain  $\epsilon$  measured by XRD using the  $\cos^2\alpha \sin^2\psi$  method, and  $C$  is the instrumental line broadening.

FE-SEM (FEI, Quanta 200F) was used to characterize the microstructures of the TiN thin films. The surface morphology (2D and 3D) of the TiN films was characterized by AFM (NT-MDT, Ntegra) to calculate the surface roughness.

## 3. Results and Discussion

XRD peaks of TiN films deposited on the Si (111) substrate in Ar+N<sub>2</sub> and pure N<sub>2</sub> atmospheres at 500 °C are shown in Fig. 1(a) and (b), respectively. The films deposited in the Ar+N<sub>2</sub> atmosphere, Fig. 1(a) exhibit a (200) preferred orientation during the initial deposition time and then change to a

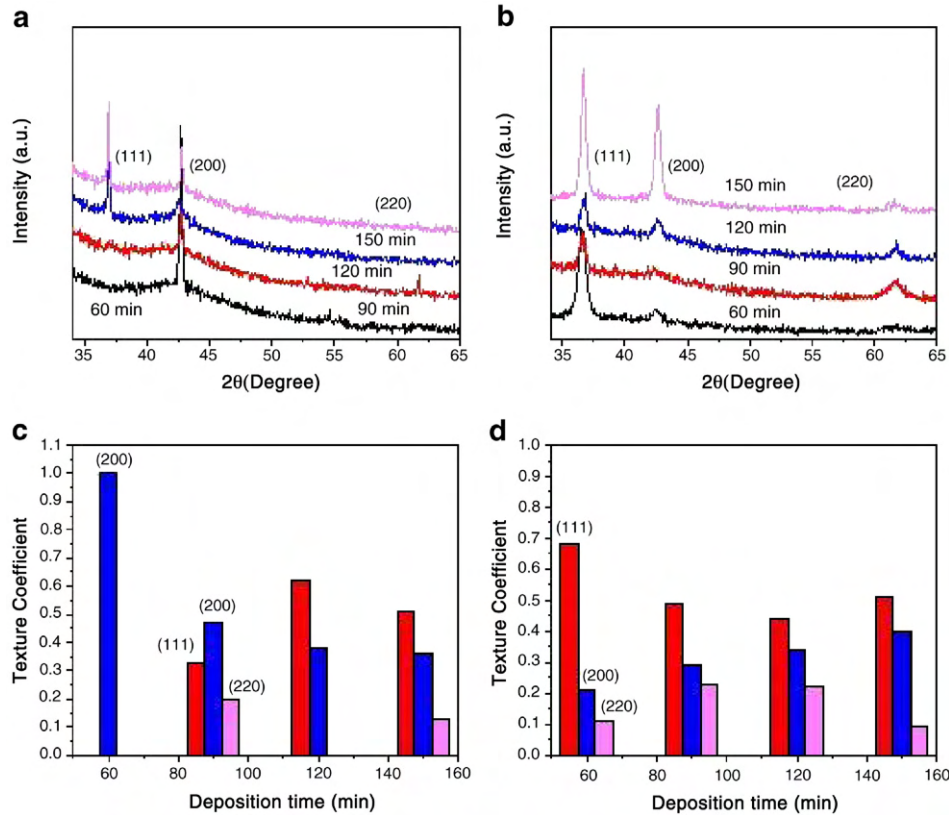


**Fig. 1** – XRD peaks and texture coefficients of TiN films deposited on Si substrate as a function of deposition time: a) and c) in an Ar+N<sub>2</sub> atmosphere, and b) and d) in an N<sub>2</sub> atmosphere.

mixture of more pronounced (111) orientation with less (200) orientation with increasing deposition time. However, the TiN thin films deposited in a pure N<sub>2</sub> atmosphere exhibit only (111) orientation and this is transformed into a mixed (200)–(111) orientation with increasing deposition time, Fig. 1(b). The texture coefficients of the TiN films as a function of deposition time are calculated from their respective XRD peaks using the following formula; the results are shown in Fig. 1(c) and (d).

$$\text{Texture coefficient}(T) = I(hkl) / [I(111) + I(200) + I(220)] \quad (2)$$

where  $hkl$  represents the (111), (200) or (220) orientations. The texture coefficients of the (200) and (111) orientation are high compared to other orientations in the TiN films deposited under Ar+N<sub>2</sub> and pure N<sub>2</sub>, respectively, during the initial deposition time. It is clear that the observed changes in textures are influenced by the high deposition temperature and time. The competition between surface energy and strain energy during film growth might contribute to these changes in preferred orientation. With an increase in deposition time and at some critical thickness, stress relaxation may reduce strain energy to a greater extent than the increase in surface energy due to the texture changes. When this occurs, an effective transition point occurs at which the texture changes. It is well known that the anisotropy of the elastic moduli will favor the growth of low strain energy-oriented grains at the expense of grains possessing higher strain energy. In addition, the substrate roughness may also affect the film texture.

From the XRD peaks, the crystallite size in the TiN films was found to be 15.34 nm and 36.66 nm after 90 min in N<sub>2</sub> and Ar+N<sub>2</sub> atmospheres, respectively. It is observed that the grain size increase with the deposition time is not high due to the formation of highly textured grains in the TiN films. Stability of the nanocrystalline TiN thin films is also partly due to the texture-controlled grain growth, in addition to the higher nucleation kinetics during the preparation of the films. The formation of nanograins in the TiN thin films reflects the influence of factors such as ion energy, ion flux, trace impurities, and textures as reported by Petrov et al. [9] and Mayrhofer et al. [19]. In the present work, the bombardment by high energy sputtered atoms may damage the growing film and create a large number of defects in the films. The density of these defects becomes very high due to the high energy of the sputtered atoms and causes repeated nucleation during film growth on the substrate. These repeated nucleation events are responsible for the formation of nanograins in the TiN thin films. Trace impurities may segregate at the grain boundaries and restrict the grain growth due to Zener drag, which is beneficial for the stability of the nanocrystalline films. During heavy ion bombardment, densification of the microstructure also occurs through the enhanced surface mobility of adatoms, which eliminates film porosity. It also increases the strain energy in the films, thereby influencing the formation of textured grains during film growth.

The microstructural morphologies of the TiN thin films deposited in Ar+N<sub>2</sub> and pure N<sub>2</sub> atmospheres at 500 °C were

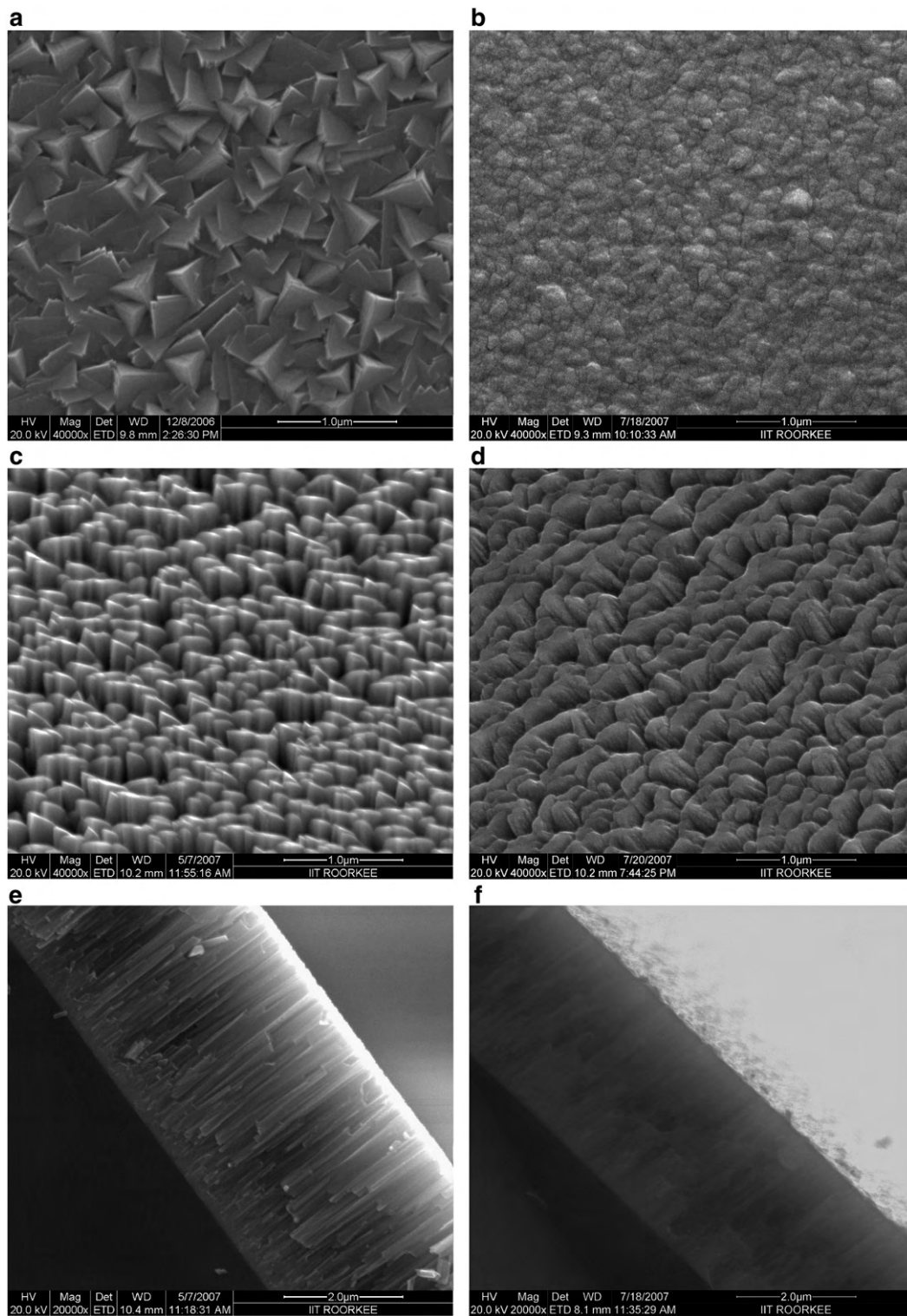


**Fig. 2** – Top surface view, 60° tilt view and cross-section FE-SEM images of TiN thin films deposited a), c) and e) in an Ar+N<sub>2</sub> atmosphere and b), d) and f) in an N<sub>2</sub> atmosphere.

characterized by FE-SEM and are shown in Fig. 2(a–d). Fig. 2(a) and (b) show surface morphologies, whereas Fig. 2(c) and (d) present images after 60° tilting. For the films deposited in the Ar+N<sub>2</sub> atmosphere, a pyramidal morphology of the grains is observed, Fig. 2(a). In the pure N<sub>2</sub> atmosphere, a columnar grain morphology is observed, Fig. 2(b). The tilted images clearly reveal the

oriented growth morphology, particularly for the film deposited in the mixed Ar+N<sub>2</sub> atmosphere. Recall from the XRD results that the initial orientation of these two films varied; for the mixed Ar+N<sub>2</sub> atmosphere the (200) orientation dominated, whereas in pure N<sub>2</sub> the initial orientation was predominantly (111). Hence, the different appearance of these two films is not surprising.

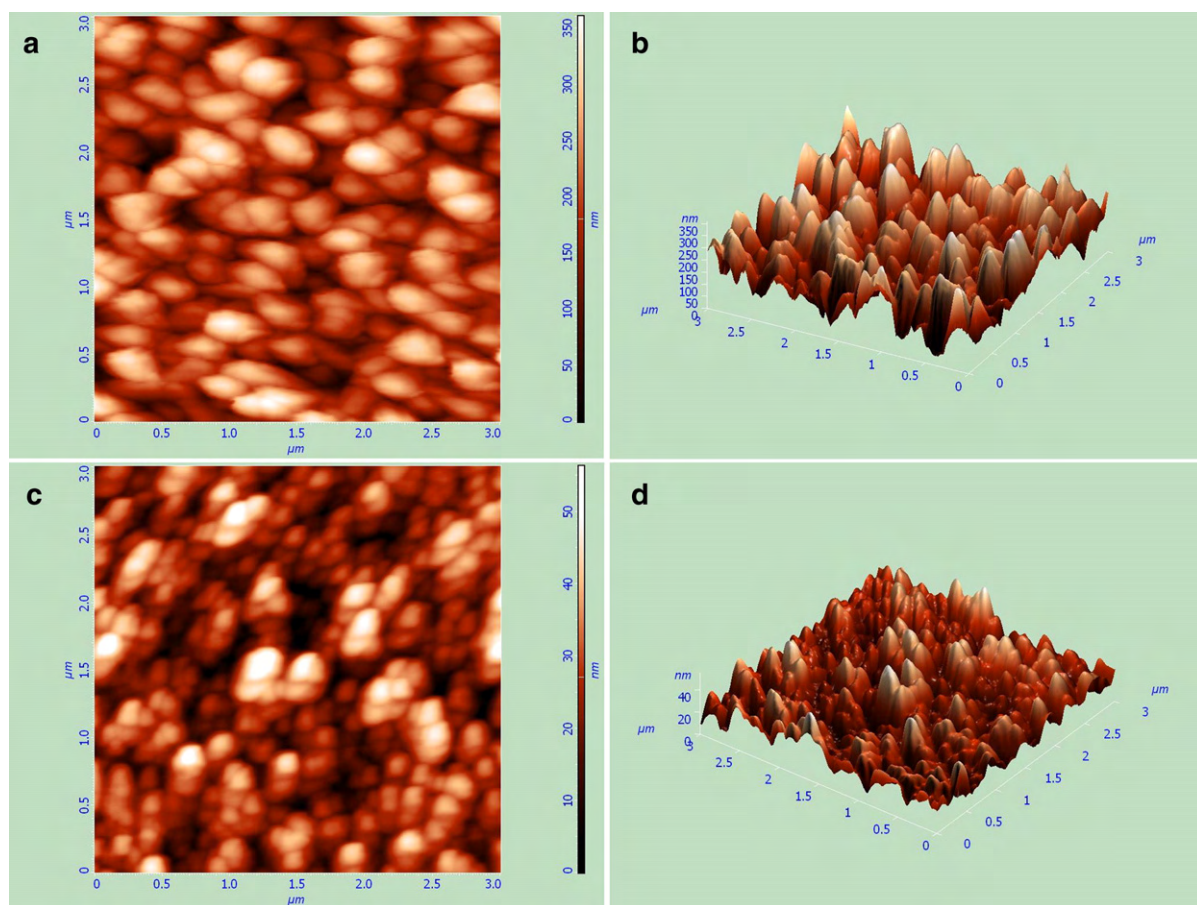


**Fig. 3**–2D and 3D AFM images of TiN films deposited a) and b) in an Ar+N<sub>2</sub> atmosphere and c) and d) in an N<sub>2</sub> atmosphere.

The preferred orientation (200) observed, in the present work, for the Ar+N<sub>2</sub> atmosphere-deposited films is different from the (111) orientation reported for films deposited similarly by Chandra et al. [16]. This is due to the difference in deposition temperature and the substrate orientation used in these cases. The pyramidal and columnar growth morphologies of the TiN films observed in this work are illustrated further in the cross-sectional FE-SEM images shown in Fig. 2(e) and (f).

Fig. 3(a–d) show the AFM surface morphology (2D and 3D) of the TiN films deposited in the Ar+N<sub>2</sub> and pure N<sub>2</sub> atmospheres at 500 °C. The difference in morphology between the two films can be inferred by comparing the 2D images in Fig. 3(a) and (c); however, a clearer comparison of the films is afforded by viewing the 3D images in Fig. 3(b) and (d). As the axis scale indicates, the overall roughness of the films prepared in the N<sub>2</sub> atmosphere (Fig. 3(d)) is less than that for the films prepared in the Ar+N<sub>2</sub> atmosphere (Fig. 3(c)).

#### 4. Conclusions

The microstructural morphologies of nanocrystalline TiN thin films deposited on Si(111) substrates were investigated in the present work. The XRD results indicate that the TiN films prepared under an Ar+N<sub>2</sub> atmosphere exhibit an initial (200) preferred orientation which gradually changes into a mixed (111)–(200) orientation with longer deposition time. However,

the initial preferred orientation for the TiN films prepared under a pure N<sub>2</sub> atmosphere is (111); this also evolves with longer deposition time to a mixed (111)–(200) orientation. These changes in texture in the TiN thin films are due to one or combination of such factors as strain energy, surface free energy, surface diffusivity and adatom mobility; the influence of each factor depends on the processing conditions. The FE-SEM analysis of the nanocrystalline TiN thin films shows that the morphology of the films deposited in the Ar+N<sub>2</sub> atmosphere has a characteristic pyramidal grain shape, whereas the films deposited in a pure N<sub>2</sub> atmosphere exhibit a more columnar-type morphology. The AFM study revealed that the overall roughness of the films prepared in the N<sub>2</sub> atmosphere is less than that for the films prepared in the Ar+N<sub>2</sub> atmosphere.

#### Acknowledgements

One of the authors, Dr. Ramesh Chandra, would like to thank DST and DRDO, in India, for their financial support to this work.

#### REFERENCES

- [1] Ma CH, Huang JH, Chen Haydn. Nanohardness of nanocrystalline TiN thin films. *Surf Coat Technol* 2006;200: 3868–75.

- [2] Ma LW, Cairney JM, Hoffman M, Munroe PR. Three dimensional imaging of deformation modes in TiN-based thin film coatings. *Thin Solid Films* 2007;515:3190–5.
- [3] Patsalas P, Charitidis C, Logothetidis S. The effect of substrate temperature and biasing on the mechanical properties and structure of sputtered titanium nitride thin films. *Surf Coat Technol* 2000;125:335–40.
- [4] Thornton JA. High rate thick film growth. *Annu Rev Mater Sci* 1977;7:239–60.
- [5] Movchan BA, Demschishin AV. Study of the structure and properties of thick vacuum condensates of nickel, titanium, tungsten, aluminium oxide and zirconium dioxide. *Phys Met Metallogr* 1969;28:83–90.
- [6] Grovenor CRM, Hentzell HTG, Smith DA. The development of grain structure during growth of metallic films. *Acta Metall* 1984;32:773–81.
- [7] Helmersson U, Sundgren JE, Greene JE. Microstructure evolution in TiN films reactively sputter deposited on multiphase substrates. *J Vac Sci Technol A* 1986;4(3):500–3.
- [8] Johannson BO, Sundgren JE, Greene JE, Rockett A, Barnett SA. Growth and properties of single crystal TiN films deposited by reactive magnetron sputtering. *J Vac Sci Technol A* 1985;3: 303–7.
- [9] Petrov I, Barna PB, Hultman L, Greene JE. Microstructural evolution during film growth. *J Vac Sci Technol A* 2003;21(5): S117–28.
- [10] Shen YG, Lu YH, Liu ZJ. Microstructure evolution and grain growth of nanocomposite TiN–TiB<sub>2</sub> films: experiment and simulation. *Surf Coat Technol* 2006;200:6474–8.
- [11] Liu Z-J, Zhang CH, Shena YG, Mai Y-W. Monte Carlo simulation of nanocrystalline TiN/amorphous SiN<sub>x</sub> composite films. *J Appl Phys* 2004;95(2):758–60.
- [12] Kim TS, Park SS, Lee BT. Characterization of nano-structured TiN thin films prepared by R.F. magnetron sputtering. *Mater Lett* 2005;59:3929–32.
- [13] Troll LE. *Transition Metal Carbides and Nitrides*. New York: Academic; 1971.
- [14] Li TQ, Noda S, Komiyama H, Yamamoto T, Ikuhara Y. Initial growth stage of nanoscaled TiN films: formation of continuous amorphous layers and thickness-dependent crystal nucleation. *J Vac Sci Technol A* 2003;21:1717–23.
- [15] Ma CH, Huang JH, Chen H. Texture evolution of transition-metal nitride thin films by ion beam assisted deposition. *Thin Solid Films* 2004;446:184–93.
- [16] Chandra R, Chawla AK, Kaur D, Ayyub P. Structural, optical and electronic properties of nanocrystalline TiN films. *Nanotechnology* 2005;16:3053–6.
- [17] Huang JH, Lau KW, Yu GP. Effect of nitrogen flow rate on structure and properties of nanocrystalline TiN thin films produced by unbalanced magnetron sputtering. *Surf Coat Technol* 2005;191:17–24.
- [18] Warren BE, Bisce. Structure of silica glass by X-ray diffraction studies. *J Am Ceram Soc* 1938;21:49–54.
- [19] Mayrhofer PH, Mitterer C, Hultman L, Clemens H. Microstructural design of hard coatings. *Prog Mater Sci* 2006;51:1032–114.